IEEE Photonics Journal
An IEEE Photonics Society Publication

Open Access

Recirculating Frequency Shifting Based Wideband Optical Frequency Comb Generation by Phase Coherence Control

Volume 7, Number 1, February 2015

Cheng Lei
Hongwei Chen, Member, IEEE
Minghua Chen, Member, IEEE
Sigang Yang, Member, IEEE
Shizhong Xie, Senior Member, IEEE

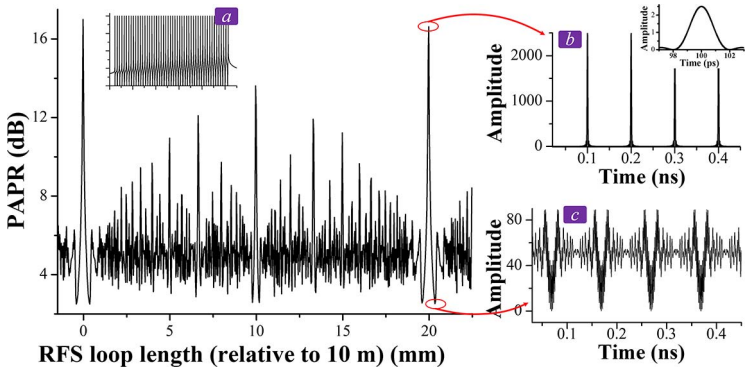

DOI: 10.1109/JPHOT.2014.2381647
1943-0655

IEEE photonics SOCIETY

IEEE

Recirculating Frequency Shifting Based Wideband Optical Frequency Comb Generation by Phase Coherence Control

Cheng Lei,[1,2] Hongwei Chen,[1,2] *Member, IEEE*, Minghua Chen,[1,2] *Member, IEEE*, Sigang Yang,[1,2] *Member, IEEE*, and Shizhong Xie,[1,2] *Senior Member, IEEE*

[1]Tsinghua National Laboratory for Information Science and Technology (TNList), Beijing 100084, China
[2]Department of Electronic Engineering, Tsinghua University, Beijing 100084, China

DOI: 10.1109/JPHOT.2014.2381647

Manuscript received October 27, 2014; accepted December 7, 2014. Date of publication December 18, 2014; date of current version January 6, 2015. This work was supported by the National Program on Key Basic Research Project (973) under contract 2012CB315703; by the Natural Science Foundation of China (NSFC) under contract 61322113, contract 61090391, contract 61132004, contract 61335002, contract 61120106001, and contract 61271134; by the young top-notch talent program sponsored by the Ministry of Organization, China; and by the Tsinghua University Initiative Scientific Research Program. Corresponding author: M. Chen (e-mail: chenmh@tsinghua.edu.cn).

Abstract: Recirculating frequency shifting (RFS) has attracted much attention for its advantages in flexible and high-quality optical frequency comb (OFC) generation. As the number of tones increases, the phase coherence of the tones plays a very important role in the stability of the generated OFC. It is found in this paper that by controlling the phase coherence of the tones, the peak-to-average power ratio (PAPR) of the generated OFC will decrease sharply. This will effectively relieve the distortion caused by fiber nonlinearity, which will enable the loop to support more tones under the condition of constant output power. Based on the phase coherence control method, a 100-tone OFC with 10-GHz frequency spacing and a single RFS loop is successfully realized.

Index Terms: Recirculating frequency shifting (RFS), optical frequency comb (OFC), phase coherence control.

1. Introduction

As an essential component of photonics research and applications, optical frequency combs (OFC) with a rectangular spectral profile have now been widely used in many areas [1]–[4]. During the past decade, with the exponential growth of bandwidth demand, high-speed wavelength division multiplexing (WDM) communication systems have been massively investigated. Due to its uniform frequency spacing and the power of its tones, OFC with a rectangular spectral profile have generally been employed as ideal carriers in WDM systems with large numbers of channels [1]–[3]. Recently, in the field of biophotonics, to simplify the system structure and increase the spectral efficiency of ultra-fast imaging systems [5], OFC with a rectangular spectral profile have been applied as the probe instead of Ti-sapphire laser because of their compact structure and rectangular spectral profile [4]. There are many available OFC generation methods, such as microresonators [6], [7], cascaded modulators, [8], [9], and optoelectronic oscillators (OEO) [10], [11]. Among them, recirculating frequency shifting (RFS) has attracted much attention for its

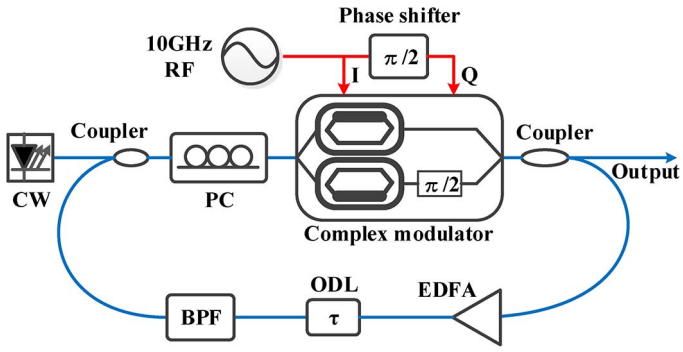

Fig. 1. System setup of the RFS loop. CW: continuous wave; RF: radio frequency; I: in phase; Q: quadrature; PC: polarization controller; BPF: band pass filter; ODL: optical delay line; EDFA: erbium-doped fiber amplifier.

advantage in generating OFC with high flexibility and a flat-top spectrum [12]–[15]. Based on the methods by which new frequencies are generated, the RFS-based OFC generators can be roughly divided into two categories. One is double sideband frequency shifting, which usually employs single or cascaded modulators (intensity modulators or phase modulators or both) in the loop. Because of the nonlinear modulating characteristic of the modulators, they are convenient for generating OFC with a wide bandwidth [12]. However, because the new frequencies are generated on both high and low frequency sidebands, the newly generated tones will inevitably overlap with existing tones. As a result, any phase or frequency differences between the overlapped tones will ultimately influence the characteristics of the generated OFC. The other method is single sideband frequency shifting. Due to the non-overlapping nature of the generation process, the good characteristics of the CW source, such as narrow linewidth, can be maintained in every tone of the generated OFC [16]. Additionally, by employing multi-loop or multi-wavelength input, the bandwidth of the generated OFC can be further increased [13]–[15]. In this paper, we will focus on RFS utilizing a single sideband frequency shifting structure.

The signal evolution of the OFC inside the loop is usually analyzed from the perspective of the spectrum, and it is believed that the tones generated by the RFS loop are frequency-locked and far less sensitive to phase noise and nonlinear propagation effects [15]. We know that if the phases of the tones in an OFC are highly synchronized (e.g., identical phases), the temporal waveform of the OFC would be pulses. When the number of tones is small, no matter what the relationship of the tones is, the pulse width will not be that narrow. In this case, the peak power of the OFC will be limited, and the influence of fiber nonlinearity would also be weak. However, as the number of tones increases, pulses may appear with a very narrow width and high peak power. In this case, the influence of fiber nonlinearity would become a key factor for the stability of the OFC. In this paper, we analyzed the stability problem of the OFC when the number of tones is large (> 50), both theoretically and experimentally, and we also proposed a phase coherence control method to increase the number of tones under the condition of constant output power. The proposed phase coherence control method is applied to stabilize the OFC when the number of tones increases, and a 100-tone OFC with 10-GHz frequency spacing and a single RFS loop is successfully realized.

2. Analysis and Experiment

The system setup of the RFS loop is shown in Fig. 1. The whole system consists of three parts: a continuous wave (CW) source, an RF signal, and a loop. The CW source provides the first wavelength and determines the starting frequency of the generated OFC. The frequency of the RF signal defines the frequency spacing of the OFC. In the loop, the complex modulator is used to realize single sideband frequency shifting, and a polarization controller (PC) is installed before the complex modulator to adjust the signal polarization to achieve maximum modulation

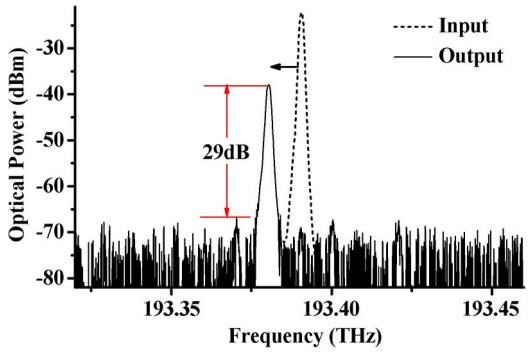

Fig. 2. Single sideband frequency shifting of a complex modulator.

efficiency. The erbium-doped fiber amplifier (EDFA) is used to compensate the transmission loss. The optical delay line (ODL) is employed to adjust the loop length, and a band pass filter (BPF) is used to confine the range of the OFC. Every time the signal passes through the complex modulator, the frequency of the signal will be shifted according to the frequency of the input RF signal, and the input CW will occupy the blank position. As a result, over time, there will be more and more frequency components, and ultimately an OFC can be generated.

As the key component of the system, the complex modulator is made up of two parallel Mach-Zehnder modulators (MZMs) and a phase shifter. By setting the bias of the two MZMs at their half-wave voltage (V_π), and introducing a $\pi/2$ phase difference between the two arms, the transfer characteristic of the complex modulator can be expressed as

$$E_{\text{out}}(t) \propto E_{\text{in}}(t) \cdot [\cos(2\pi \cdot f_{\text{RF}} \cdot t) + j \cdot \sin(2\pi f_{\text{RF}} \cdot t)] = E_{\text{in}}(t) \cdot e^{j \cdot 2\pi \cdot f_{\text{RF}} \cdot t}. \quad (1)$$

In (1), E_{in} and E_{out} express the input and output signal of the modulator, respectively, and f_{RF} denotes the frequency of the RF signal. It is clear from the equation that after the complex modulator, the center frequency of the input signal will be shifted by f_{RF}. The single sideband frequency shifting realized in the experiment is shown in Fig. 2.

In Fig. 2, the dotted line represents the spectrum of the input CW signal, and the solid line represents the spectrum of the shifted signal. Due to the single sideband frequency shifting characteristic of a complex modulator, the frequency of the input signal is shifted without any residual or mirror components. Due to the power loss of the complex modulator, the power of the frequency-shifted signal is approximately 15 dB lower than the input CW, which can be compensated by the EDFA in the loop. During the frequency shifting period, noise will inevitably accumulate. Therefore, as shown in Fig. 2, the tone-to-noise ratio (TNR) of the frequency-shifted signal, which is 29 dB here, will limit the possible number of tones in the generated OFC.

In the loop, the tones are shifted in one direction so that every tone newly generated is moved toward the frequency of its adjacent tone. As the tones are generated by frequency shifting but not oscillation, when we analyze the signal evolution inside the loop, we can ignore the loop structure and treat it as straight-line transmission, as is commonly done in loop transmission experiments. This is coincident with the comb-like spectrum of the output signal and also makes the analysis much simpler. However, from the perspective of the whole system, once the output of the RFS loop is a stable OFC, all the tones simultaneously exist in the loop. Additionally, the tones are completely frequency-locked, creating a similar situation as in a mode lock laser (MLL). Hence, if the phases of the tones in the loop satisfy the time condition, the temporal waveform would be pulses, as happens in an MLL loop. It can be predicted that as the number of coherent tones becomes larger, the width of the pulses will become narrower. Under the condition of constant optical power, the peak power of the pulses will also sharply increase. As high peak power induces severe fiber nonlinearity, the phase coherence of the tones is an important limitation to increasing the number of tones of the OFC.

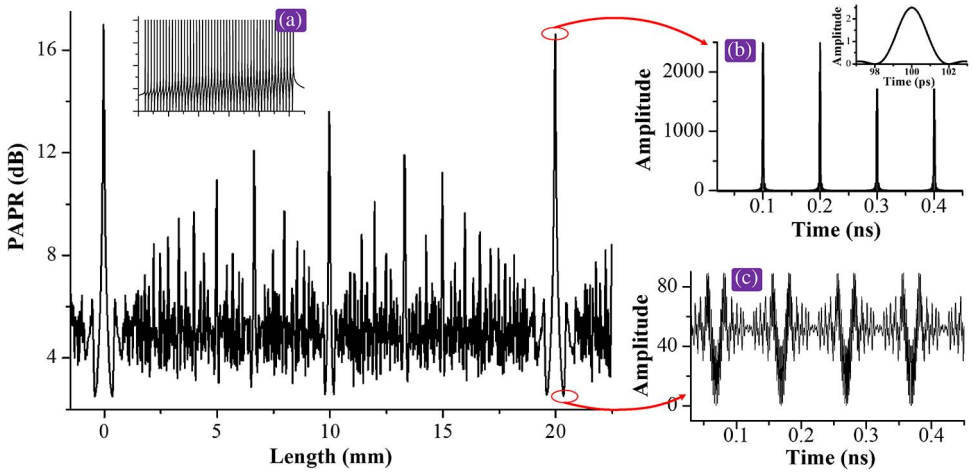

Fig. 3. The relationship between the signal PAPR and the length of the loop. The length of the loop in the horizontal axis is a relative value compared to 100 m. (a) Spectrum of the 50-tone OFC. (b) Temporal waveform of an OFC with high PAPR. (b) Temporal waveform of an OFC with low PAPR.

As Fig. 1 shows, the easiest way to influence the phase relationship between the tones is to adjust the length of the loop. This process is mathematically expressed below. As, in the proposed scheme, the tones of the OFC are generated by frequency shifting but not oscillation, the dispersion will only add an extra phase to the tones but not affect the generation of the OFC. We therefore neglected dispersion in the analysis below. Assuming the frequency of the CW source is ω_0, the frequency of the RF signal is ω_{RF}, the length of the loop is L, and the speed of light in the fiber is c/n, where n is the effective refractive index of the fiber and c the speed of light in vacuum. If there is a total of N tones in the generated OFC, the first tone, which is the closest to the CW, can be expressed as

$$f_1 = e^{j\omega_0 t} \cdot e^{j\omega_{RF} t}. \tag{2}$$

According to the signal transmission character in the loop, the m-th nearest tone to the CW, which can be noted as f_m, will travel $m-1$ rounds more than the first tone f_1. Similar to (2), we can express f_m as

$$f_m = e^{j\omega_0 t} \cdot e^{j\omega_{RF} \cdot m \cdot t} \cdot e^{j\cdot(m-1)\cdot\frac{n\cdot L}{c}\cdot\omega_0} \cdot e^{j\cdot\frac{n\cdot L}{c}\cdot\omega_{RF}\cdot\sum_{k=0}^{m-1} k}. \tag{3}$$

It is clear in (3) that when the frequency of the RF is fixed, the phases of the tones are determined only by the length of the loop. To better express the relationship between the phases of the tones and the temporal waveform of the OFC, we calculated the relationship between the peak to average power ratio (PAPR) of the generated 50-tone OFC and the length of the loop, as shown below.

To show more detail, in Fig. 3, the length of the loop on the horizontal axis is a relative value compared to 100 m, which is a typical length of an RFS loop [17]. It is clear in Fig. 3 that as the length of the loop changes, the PAPR of the OFC can vary from less than 3 dB to as high as 17 dB. It must be emphasized that during the whole process of changing the length of the loop, the spectrum of the output is always an OFC, as Fig. 3(a) shows. For the temporal waveform of the OFC, we take two typical points, the maximum and minimum values of the PAPR, as an example, which is noted by the red circles in Fig. 3.

When the PAPR reaches its maximum value, which is 17 dB in Fig. 3, the temporal waveform of the OFC is pulses, as shown in Fig. 3(b). We can see in the zoomed-in insert that the width of the pulse is only approximately 2 ps. Comparing Fig. 3(a) with (b), we see that at this time, the phase coherence of the tones is just like the situation in an MLL; therefore, the temporal waveform is narrow pulses. If the average power of the signal inside the loop is 20 dBm (this is

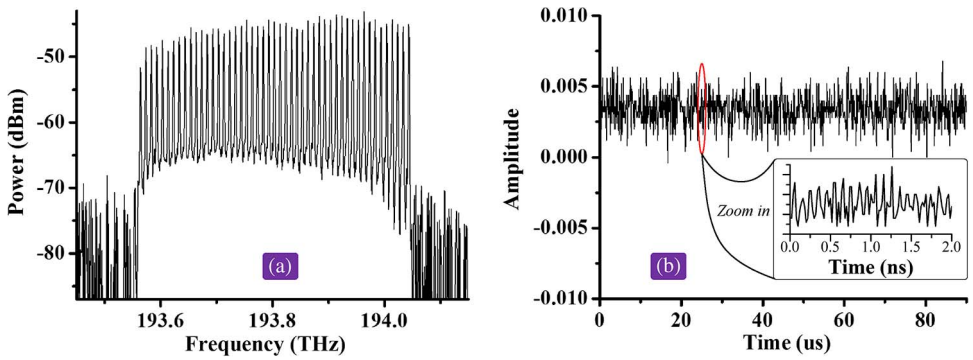

Fig. 4. Spectrum (a) and temporal waveform (b) of the signal when it is a stable OFC in the frequency domain.

a typical value used in the experiment, and we will show this in the following part of the paper) considering the high PAPR, the peak power of the pulses will be as high as 37 dBm. This is high enough to induce very severe nonlinearity in the fiber loop. Therefore, we can predict that in this situation, the OFC and pulses shown in Fig. 3(a) and (b) can exist only mathematically but will be distorted by severe nonlinearity in real systems.

On the other hand, when the PAPR reaches its minimum value, which is 2.5 dB in Fig 3, the temporal waveform of the OFC is shown in Fig. 3(c). In this situation, we can see that although the spectrum of the signal is still a stable OFC, the temporal waveform of the signal is just like noise (because the phases of the tones are coherent, the signal in Fig. 3(c) is periodic). This is analogous to situation where a set of free-run CW sources is coupled together. Compared with the situation with high PAPR, this is more likely to stably exist in the loop for a long period of time.

In addition to the maximum and minimum points, there are also other peaks and valleys in Fig. 3. The general principle is that adjusting the length of the loop to lower the PAPR as much as possible will help relieve fiber nonlinearity, which, in the end, will stabilize the output OFC.

To experimentally verify the conclusion above, we constructed a system as shown in Fig. 1. The frequency of the RF signal is 10 GHz, and the bandwidth of the BPF is set to 4 nm (500 GHz @ 1550 nm); therefore, in theory, there should be 50 tones in the generated OFC. To compensate for the loss in the loop and guarantee a higher SNR of the tones, the average power in the loop is approximately 20 dBm. We fed the output signal to a spectrum analyzer with a resolution of 0.01 nm and observed the spectrum. By carefully adjusting the ODL, we were able to obtain a stable 50-tone OFC on the screen of the spectrum analyzer, as shown in Fig. 4(a). We then used a photodetector (bandwidth 40 GHz) to transfer the signal into the electrical domain and sampled it using a Tektronix digital phosphor oscilloscope (DPO72004B, sample rate 50 GS/s, bandwidth 20 GHz). The temporal waveform and the zoom-in detail are shown in Fig. 4(b). It is clear that when the output signal of the RFS loop is a stable OFC, its spectrum and temporal waveform [see Fig. 4(a) and (b)] are quite coincident with Fig. 3(a) and (c), with a stable OFC in the frequency domain and a noise-like waveform in the time domain. As the length of the loop is relatively long (100 m), environmental factors such as vibration and thermal effects will have a strong influence on the system. As Fig. 4(b) shows, compared with Fig. 3(c), the temporal waveform here is more noise-like than periodic.

If we continue to carefully adjust the ODL, besides the result shown in Fig. 4, we could also see fleeting pulses in the time domain. To better observe the signal, we used a Tektronix optical sampling oscilloscope (TDS8200, bandwidth 60 GHz) to capture the pulses. Fig. 5(b) shows the captured pulses, which have a repetition rate of 10 GHz, which is coincident with the frequency of the stimulating RF signal. However, in this situation, the pulses are not stable, and we sometimes obtain only a noise-like signal, as shown in Fig. 4(b) on the screen. We also measured the spectrum of the signal in this situation. As shown in Fig. 5(a) (black), in this situation, the spectrum of the signal is no longer a stable OFC and there are some places where the spectrum

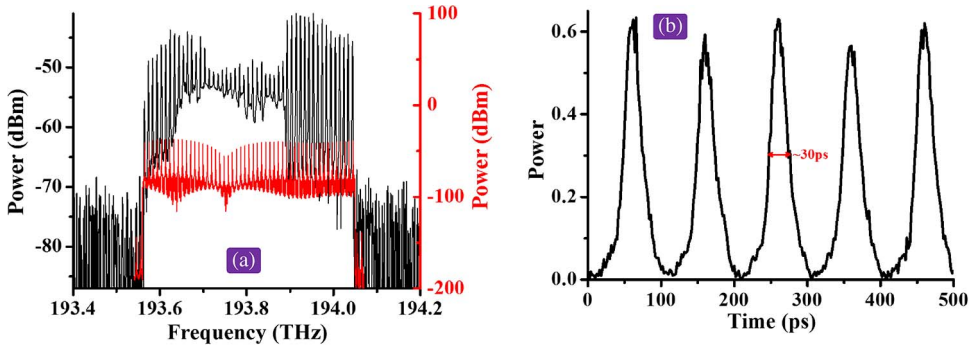

Fig. 5. Spectrum (a) and temporal waveform (b) of the signal when pulses can be observed.

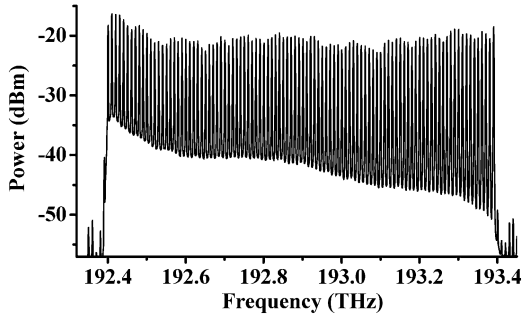

Fig. 6. Spectrum of the 100-tone 10 GHz OFC generated by a single RFS loop.

was clearly distorted. As the sweeping time of the spectrum analyzer is relatively long (~1 s), what we get in Fig. 5(a) (black) is actually the "samples" of the situations during the sweeping period. We find that sometimes the spectrum is comb-like and sometimes the spectrum is disordered. When we adjust the ODL to the point as shown in Fig. 3(b), there would theoretically be pulses in the time domain, but narrow pulses mean a high peak power, which would induce more severe fiber nonlinearity. In this situation, the self-phase modulation (SPM) would be the main factor. Under the influence of nonlinearity, the width of the pulses will be broadened and, as the peak power of the pulse goes down, the nonlinearity effect will also dissipate. Stimulated by the input CW and RF signal, tones with better SNR performance will be formed.

We simulated the signal evaluation under the influence of fiber nonlinearity (mainly SPM). In the simulation, the input signal is optical pulses with 50 tones with spectral and temporal waveforms as shown in Fig. 3(a) and (b). The peak power of the pulses is 4 W, and the fiber length is 100 m. The spectrum of the signal after fiber transmission is the red curve shown in Fig. 5(a). Comparing the simulated (red) and captured (black) spectra in Fig. 5, we can find that when the peak power of the OFC increases, under the influence of fiber nonlinearity, the power of the spectrum will decrease due to spectrum splitting, and the noise floor will rise, as well [18]. At the same time, we notice that, in Fig. 5(b), the width of the pulses is approximately 30 ps, which is much wider than the simulation result in Fig. 3(b). This also implies that pulses with a very narrow width (high peak power) cannot stably exist in the loop. The simulation results are coincident with what we observed in the experiment and also support our explanation above.

Based on the theoretical and experimental analyses above, we further increased the bandwidth of the BPF in the RFS loop to 8 nm (1 THz @ 1550 nm). The proposed phase coherence control method was applied to stabilize the OFC when the number of tones increased. As shown in Fig. 6, a 100-tone OFC with 10-GHz frequency spacing and a single RFS loop was successfully realized. The power fluctuation of the 100-tone OFC was less than 6.5 dB, and the TNR was greater than 17 dB.

3. Conclusion

In this paper, the relationship between the phase coherence of tones and the spectrum of the OFC generated by a RFS loop is investigated for the first time. Through theoretical analysis and experimental verification, we found that as the number of tones in the OFC increases, the phase coherence of the tones significantly influences the peak power of the OFC. Excessively high peak power induces severe fiber nonlinearity, which distorts the generated OFC. As one of the most convenient solutions, the phase coherence of the tones can be adjusted by changing the length of the RFS loop. Adjusting the length of the loop to lower the peak power of the OFC will make the RFS loop support more tones under the same average output power with good SNR performance. Based on this phase coherence control method, a 100-tone OFC with 10-GHz frequency spacing and a single RFS loop was successfully realized.

References

[1] G. Gavioli *et al.*, "Ultra-narrow-spacing 10-channel 1.12 Tb/s D-WDM long-haul transmission over uncompensated SMF and NZDSF," *IEEE Photon. Technol. Lett.*, vol. 22, no. 19, pp. 1419–1421, Oct. 2010.
[2] Y. Ma, Q. Yang, Y. Tang, S. Chen, and W. Shieh, "1-Tb/s single-channel coherent optical OFDM transmission over 600-km SSMF fiber with subwavelength bandwidth access," *Opt. Exp.*, vol. 17, no. 11, pp. 9421–9427, May 2009.
[3] C. Lei *et al.*, "1-Tb/s WDM-OFDM-PON system with subband access scheme and flexible subcarrier-level bandwidth allocation," *IEEE Photon. J.*, vol. 5, no. 1, Feb. 2013, Art. ID. 7900208.
[4] H. Chen *et al.*, "Multiwavelength time-stretch imaging system," *Opt. Lett.*, vol. 39, no. 7, 2014, pp. 2202–2205.
[5] K. Goda, K. K. Tsia, and B. Jalali. "Serial time-encoded amplified imaging for real-time observation of fast dynamic phenomena" *Nature*, vol. 458, no. 7242, pp. 1145–1149, 2009.
[6] P. Del'Haye *et al.*, "Optical frequency comb generation from a monolithic microresonator," *Nature*, vol. 450, no. 7173, pp. 1214–1217, 2007.
[7] T. J. Kippenberg, R. Holzwarth, and S. A. Diddams, "Microresonator-based optical frequency combs," *Science*, vol. 332, no. 6029, pp. 555–559, 2011.
[8] Y. Dou, H. Zhang, and M. Yao, "Generation of flat optical-fequency comb using cascaded intensity and phase modulators," *IEEE Photon. Technol. Lett.*, vol. 24, no. 9, pp. 727–729, 2012.
[9] T. Sakamoto,T. Kawanishi, and M. Izutsu, "Asymptotic formalism for ultraflat optical frequency comb generation using a Mach-Zehnder modulator," *Opt. Lett.*, vol. 32, no. 11, pp. 1515–1517, 2007.
[10] M. Wang and J. Yao, "Tunable optical frequency comb generation based on an optoelectronic oscillator," *IEEE Photon. Technol. Lett.*, vol. 25, no. 21, pp. 2035–2038, 2013.
[11] T. Sakamoto, T. Kawanishi, and M. Izutsu, "Optoelectronic oscillator using a LiNbO3 phase modulator for self-oscillating frequency comb generation," *Opt. Lett.*, vol. 31, no. 6, pp. 811–813, 2006.
[12] J. Zhang, N. Chi, and J. Yu, "Generation of coherent and frequency-lock multi-carriers using cascaded phase modulators and recirculating frequency shifter for Tb/s optical communication," *Opt. Exp.*, vol. 19, no. 14, pp. 12 891–12 902, 2011.
[13] J. Zhang *et al.*, "Stable optical frequency-locked multicarriers generation by double recirculating frequency shifter loops for Tb/s communication," *J. Lightw. Technol.*, vol. 30, no. 24, pp. 3938–3945, 2012.
[14] J. Zhang *et al.*, "Improved multicarriers generation by using multifrequency shifting recirculating loop," *IEEE Photon. Technol. Lett.*, vol. 24, no. 16, pp. 1405–1408, 2012.
[15] J. Zhang *et al.*, "Multichannel optical frequency-locked multicarrier source generation based on multichannel recirculation frequency shifter loop," *Opt. Lett.*, vol. 37, no. 22, pp. 4714–4716, 2012.
[16] Y. Yu *et al.*, "Generation and noise analysis of a wide-band optical frequency comb based on recirculating frequency shifter," *Chin. Opt. Lett.*, vol. 12, no. 10, 2014, Art. ID. 100601.
[17] C. Lei, H. Chen, M. Chen, S. Yang, and S. Xie, "High-speed laser scanner with tunable scan rate, wavelength resolution and spectral coverage," presented at the CLEO: Applications Technol. Opt. Soc. Amer., San Jose, CA, USA, 2013, JM3O-3.
[18] G. P. Agrawal, *Nonlinear Fiber Optics*, 3rd ed. New York, NY, USA: Academic, pp. 97–108.